



Cellulose nanofibers isolation and characterization from ramie using a chemical-ultrasonic treatment

Edi Syafri, Anwar Kasim, Hairul Abral & Alfi Asben

To cite this article: Edi Syafri, Anwar Kasim, Hairul Abral & Alfi Asben (2019) Cellulose nanofibers isolation and characterization from ramie using a chemical-ultrasonic treatment, Journal of Natural Fibers, 16:8, 1145-1155, DOI: [10.1080/15440478.2018.1455073](https://doi.org/10.1080/15440478.2018.1455073)

To link to this article: <https://doi.org/10.1080/15440478.2018.1455073>



Published online: 29 Mar 2018.



Submit your article to this journal [↗](#)



Article views: 106



View related articles [↗](#)



View Crossmark data [↗](#)



Citing articles: 7 View citing articles [↗](#)



Cellulose nanofibers isolation and characterization from ramie using a chemical-ultrasonic treatment

Edi Syafri^a, Anwar Kasim^b, Hairul Abral^c, and Alfi Asben^b

^aDepartment of Agricultural Technology, Politeknik Pertanian, Payakumbuh, Indonesia; ^bDepartment of Agriculture Product Technology, Universitas Andalas, Limau Manis, Indonesia; ^cDepartment of Mechanical Engineering, Universitas Andalas, Kampus Limau Manis, Indonesia

ABSTRACT

The novelty of this work lies in isolating cellulose nanofibers from ramie (*Boehmerianivea* (L.) Gaud) using chemical-ultrasonication treatment. The cellulose nanofibers were successfully isolated from ramie with a diameter and length of 9.9–89.1 nm and 1 μm , respectively. The samples were characterized by scanning electron microscopy, transmission electron microscopy, particle size analysis, Fourier transform infrared spectroscopy, X-ray diffraction analysis, and thermogravimetric analysis. Indeed, there is a decrease in the hemicellulose and lignin content while the cellulose content increases due to the pulping and bleaching processes. The chemical-ultrasonication treatment results in a high yield of cellulose nanofibers (89.35%).

摘要

本文的新颖之处在于从苧麻中分离纤维素纳米纤维 (*Boehmerianivea* (L.) Gaud) 使用化学超声可听化处理。分别从直径为9.9~89.1 nm和1 μm 的苧麻中分离出纤维素纳米纤维。通过扫描电镜、透射电镜、粒度分析、傅立叶变换红外光谱、X射线衍射分析、热重分析等手段对样品进行了表征。事实上,半纤维素和木质素含量减少,而纤维素含量的增加由于制浆和漂白过程。在高产量的纤维素纳米纤维化学超声治疗结果(89.35%)。

KEYWORDS

Ramie; cellulose; nanofibers; natural fibers; chemical treatment; ultrasonication



关键词

纤维素; 纳米纤维; 天然纤维; 化学处理; 超声波处理

Introduction

The depletion of petroleum-based resources and concerns over environmental issues such as climate change and global warming have led to the development natural fibers instead of synthetic fibers (Damanik et al. 2017; Silitonga et al. 2017; Vignesh, Balaji, and Karthikeyan 2016). This is largely due to the fact that natural fibers are relatively inexpensive, lightweight, biodegradable, and environmentally friendly, considering that the production of synthetic fibers uses significant amounts of energy and synthetic fabrics contribute significantly to marine plastic pollution. In addition, natural fibers have high specific strength (Abral et al. 2014; Senthamarai kanna n et al. 2016; Wahono et al. 2018). With the advent of renewable energy-based technologies, it is now possible to replace synthetic fibers such as glass fibers with natural fibers in reinforced composites, which will help mitigate environmental issues in the long term (Manimaran et al. 2017; Cadena et al. 2017; Syafri et al. 2017).

A large number of studies have been carried out to isolate highly purified cellulose nanofibers (CNFR) from various plants such as ramie (Lu and Cao, and Xiaodong 2006), wood (Abe, Iwamoto, and Yano 2007), sisal (Morán et al. 2008), pineapple leaves (Cherian et al. 2010), *Imperatabrasiliensis* Trin. (Brazilian satintail) (Benini et al. 2016), and *Ipomoea staphylina* (Santhanam et al. 2016).

CONTACT Edi Syafri  edisyafr11@gmail.com  Department of Agricultural Technology, Politeknik Pertanian, Payakumbuh, West Sumatra 26271, Indonesia.

Color versions of one or more of the figures in the article can be found online at www.tandfonline.com/wjnf.

Pretreatment and nanofibrillation are necessary to produce CNFR from plant fibers. Various pretreatment processes have been implemented to remove noncellulosic materials from the plant fibers such as alkali treatment (Yongvanich 2015), enzymatic pretreatment (Tibolla et al. 2017), ionic liquids (Han et al. 2013), TEMPO (2,2,6,6-tetramethylpiperidine-1-oxyl)-mediated oxidation (Quintana et al. 2017), and steam explosion treatment (Chirayil et al. 2014). Following this, nanofibrillation technologies such as grinders and ultrasonication (Khawas and Deka 2016) were used to isolate the nanofibrils from the purified cellulose fibers.

High-intensity ultrasonication has been proposed as a nanofibrillation method in order to isolate microfibrils and nanofibers from cellulose fibers (Khawas and Deka 2016). The powerful mechanical oscillating power and high-intensity ultrasound waves produce implosive collapse of bubbles in liquids. This phenomenon is known as acoustic cavitation, which provides 10–100 kJ mol⁻¹ of energy and is capable of breaking down hydrogen bonds. When the rapidly forming and collapsing microbubbles interact with one another and collide with the cellulose surface, they erode and denude the surface, resulting in fibrillation and formation of nanofibers (Chen et al. 2011a; Kusumo et al. 2017).

Owing to the advantages of natural fibers and benefits of high-intensity ultrasonication treatment, in this study, an attempt has been made to isolate CNFR were isolated from ramie (*Boehmerianivea* (L.) Gaud) by means of chemical-ultrasonication treatment in order to enhance the effectiveness of hemicellulose and lignin removal and attain a high yield of CNFR. The samples were characterized by scanning electron microscopy (SEM), transmission electron microscopy (TEM), particle size analysis (PSA), Fourier transform infrared (FTIR) spectroscopy, X-ray diffraction (XRD) analysis, and thermogravimetric analysis (TGA). It is believed that the findings presented in this article will provide insight on the use of chemical-ultrasonication treatment in the production of CNFR.

Materials and methods

Materials

The ramie plants were collected from Politeknik Pertanian Payakumbuh, Indonesia, located ~700 m above sea level. The ramie fibers were collected by removing the bark from the main stems of the plant by a process known as decortication. The following reagents were used in this process: (1) sodium hydroxide (NaOH, purity > 98%), (2) potassium hydroxide (KOH, purity: 99%), (3) sodium chlorite (NaClO₂), and (4) acetic acid (CH₃COOH).

Isolation

The ramie fibers were first cut into small pieces (length: 10–20mm) and dried under the sun for 3 days in order to reduce their water content 9–11%. Next, 500 g of dried ramie fibers and 18 (w/v)% of NaOH were added into a digester and the ramie fibers were cooked for 120 min at a temperature of 170°C and pressure of 7–9 bar in order to remove hemicellulose and lignin (Syafri et al. 2016). After the pulping process (PR), the ramie fibers were washed with distilled water until the pH was neutral (pH = 7). The bleaching process was carried out in two stages in order to remove residual hemicellulose and lignin from the ramie fibers. In the first stage, the 5 (w/v)% of NaClO₂ and 3 mL of CH₃COOH were added into the pulp and the bleaching process was conducted for 120 min at 170°C until the pH was slightly acidic (pH = 5). The pulp remaining after the first stage of bleaching process was washed with distilled water until the pH value was neutral (pH = 7). Next, the second stage of the bleaching process (BR) was carried out using 4 (w/v)% of KOH for 60 min at 80°C. The chemically purified cellulose ramie fibers were loaded with 2(w/v)% of deionized water and sonicated using a 1.5 cm cylindrical probe (frequency: 22 kHz, output power: 400W) for 60 min at a temperature of 70°C. [Figure 1](#) shows the flowchart of the steps involved to isolate the CNFR from

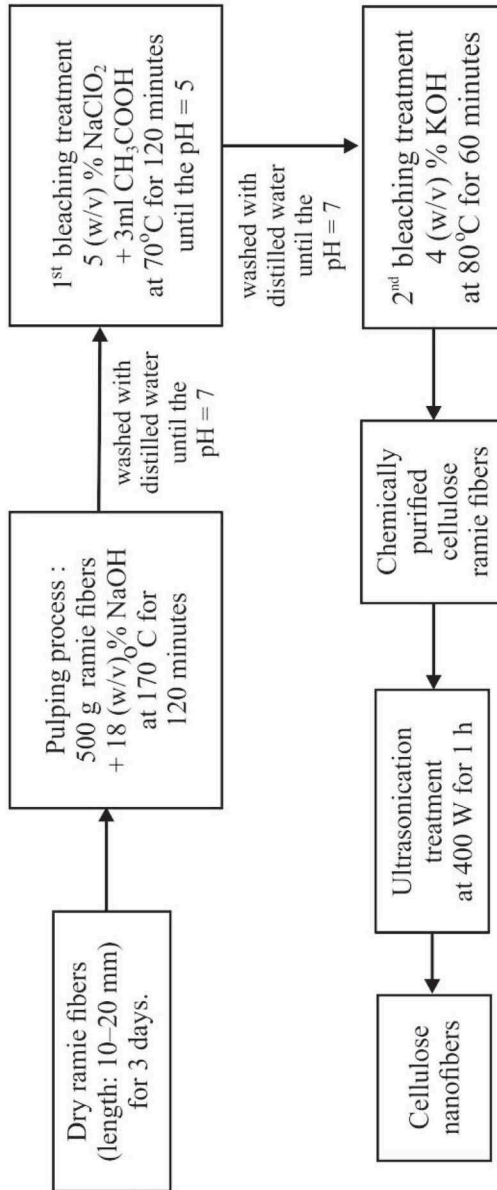


Figure 1. Flowchart of the steps involved to isolate the cellulose nanofibers from ramie by chemical-ultrasonication treatment.

ramie. The yield of the CNFR was determined using Eq. (1) based on the weight of the CNFR and weight of native cellulose fibers determined from thermogravimetric measurements:

$$\text{Yield}(\%) = \left(\frac{\text{Weight of cellulose nanofibers}}{\text{Weight of native cellulose fibers}} \right) \times 100 \quad (1)$$

Characterization

The chemical compositions of the raw ramie fibers (RR), ramie fibers after PR, and ramie fibers after BR were measured in accordance with the ASTM D 1104–56 standard (hemicellulose), TAPPI T9m-54 standard (cellulose) and TAPPI T3m-54 standard (lignin). FTIR spectroscopy analysis was performed using Perkin Elmer FrontierTM FTIR spectrometer with a wavelength range of 400–4,000 cm^{-1} . The crystallinity of the samples was determined from the X-ray diffractograms measured over a 2θ range of 2–100° and time step of 20°/min. PANalytical X-ray diffractometer with Cu-K α radiation ($\lambda = 1.5406 \text{ \AA}$, voltage = 40 kV, current = 30 mA) was used for the XRD analysis. The crystallinity index (CI) was calculated based on the intensity of the 002 peaks (I_{002} , $2\theta = 22.6^\circ$) and the minimum intensity between the 200 and 110 peaks (I_{am} , $2\theta = 18^\circ$) using the method of Segal et al. (Gopinath et al. 2016; Segal et al. 1959), which is given by Eq. 2. Here, I_{002} represents the intensity of the crystalline and amorphous phases whereas I_{am} represents the intensity of the amorphous phase.

$$CI (\%) = \left(\frac{I_{002} - I_{am}}{I_{002}} \right) \times 100 \quad (2)$$

The thermal degradation characteristics of the CNFR were assessed using a thermogravimetric analyzer (Model: TGA4000, PerkinElmer, USA) within a temperature range of 50–500°C at a heating rate of 10°C/min and nitrogen flow of 60mL/min. The surface morphologies of the ramie fibers (RR, PP, and BR samples) were observed using a SEM (Model: S-3400N, Hitachi, Ltd., Japan) at 20 kV. The specimens were prepared for SEM by placing the chemically treated ramie fiber particles on to a double-sided carbon tape in high vacuum mode. TEM (Model: JEM 1400, JEOL, USA) was used to examine the surface morphology of the CNFR. The specimen was prepared by placing a few drops of the ultrasonicated CNFR suspension onto a thin carbon-coated copper grid. The CNFR suspension was left to dry at room temperature and the sample was then observed under the TEM at an accelerated voltage of 80 kV. A particle size analyzer (Model: DelsaTM Nano C, Beckman Coulter Inc., USA) was used to measure the diameter of the CNFR. Photon correlation spectroscopy was used to determine the particle size by measuring the degree of fluctuations in the intensity of the laser beam spread due to the particles suspended in the liquid. The samples were measured under the following settings: temperature: (1) temperature: 25°C, (2) viscosity: 0.88 cP, (3) scattering intensity: 9581 cps, (4) refractive index: 1.3332, and (5) time: 2 min. DelsaTM Nano software was used to process the particle size data.

Results and discussion

Chemical compositions of the ramie fibers

Chemical processes (pulping and two-stage BRs) were used to remove hemicellulose, lignin, and other impurities from the RR fibers, producing chemically purified cellulose fibers. The chemical compositions of the RR, PR, and BR samples are presented in Table 1. It can be seen that the

Table 1. Chemical compositions of the raw ramie fibers (RR), ramie fibers after the pulping process (PR), and ramie fibers after the two-stage bleaching process (BR).

Sample	Holocellulose (wt%)	Hemicellulose (wt%)	Cellulose (wt%)	Lignin (wt%)
RR	79.45	9.63	69.83	3.98
PR	92.09	7.52	84.56	1.97
BR	93.09	6.42	86.69	1.76

holocellulose content increases from 79.45wt% (RR) to 93.09wt% (BR) due to the pulping and BRs, which corresponds to an increase of 17.16%. In contrast, the hemicellulose content decreases from 9.63wt% (RR) to 6.42wt% (BR), which corresponds to a decrease of 50%. Likewise, the lignin content decreases from 3.98wt% (RR) to 1.76wt% (BR). The results indicate that the NaClO_2 , CH_3COOH , and KOH effectively remove most of the hemicellulose and lignin present in the RR fibers. This is likely due to the destruction of the cell wall structure during the PR (George and Narayanankutty 2016). The lignin reacts with NaClO_2 , forming a soluble lignin chloride compound (Chirayil et al. 2014). The remaining hemicellulose and lignin are removed by the NaClO_2 and KOH during the two-stage BR. The lignin, hemicellulose, and cellulose content after the BR are 1.76 wt%, 6.42 wt%, and 86.69 wt%, respectively.

Surface morphologies of the chemically purified cellulose fibers

Figure 2a, b, and c show the SEM images of the RR, PR, and BR samples, respectively, whereas Figure 2d shows the TEM image of the CNFR sample obtained from chemical-ultrasonication treatment. It can be seen from Figure 2a that the RR fibers are composed of large bundles (diameter: 70–150 μm) and the intact structures are covered with other impurities such as hemicellulose, lignin, pectin, and waxy substances. The morphological structure of the ramie fibers after PR differs significantly from that of the RR fibers. After 120 min of PR, the fiber bundles were separated into individual microfibers, as shown in Figure 2b. The termination of the amorphous region is marked by a significant decrease in the diameter of the ramie fibers from 70–150 μm to 20–50 μm .

After the two-stage BR, the microfibers were separated into individual micro-cellulose fibers, as shown in Figure 2c. The average diameter of micro-cellulose fibers reduces further to 1–5 μm . It can be observed that the surface of the micro-cellulose fibers appears to be smoother. The results indicate that the removal of impurities such as lignin and hemicellulose by delignification and BRs significantly reduces the diameter of the ramie fibers from 20–50 μm to 1–5 μm as well as disintegrate the fiber bundles into individual micro-cellulose fibers. The chemical treatment (pulping and BRs) results in separation of fasciculus due to the removal of lignin in the middle lamella which leads to disintegration of the compact ramie structure. It is evident that the chemical treatment is effective for defibrillation of the ramie fibers.

The morphological structure of the CNFR is indeed different from the others, as shown in Figure 2d. It can be seen that the individual long fibers are tangled together, forming web-like structure. It is apparent that the nanofibrillation forces introduced by ultrasonication breaks down the hydrogen bonds in order to defibrillate the cellulose fibers obtained from the chemical treatment. This disintegrates the micro-fibers to form nanofibrils (Khawas and Deka 2016). The nanofibrils are tangled, forming a large aggregated bundle with a diameter and length of ~20–50 nm and 1 μm , respectively.

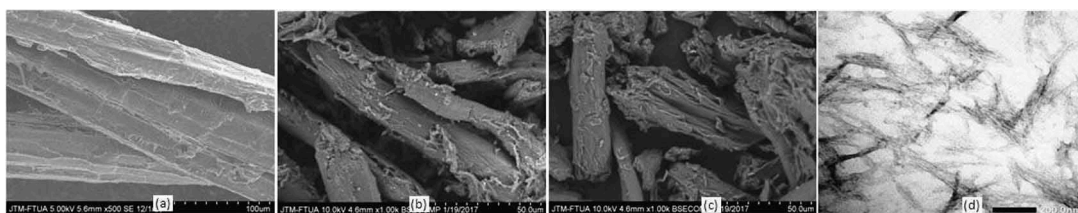


Figure 2. SEM images of the (a) raw ramie fibers (RR), (b) ramie fibers after the pulping process (PR), and (c) ramie fibers after the two-stage bleaching process (BR), and (d) TEM image of the cellulose nanofibers (CNFR).

PSA

Based on the results obtained from PSA, the CNFR has a uniform diameter within a range of 9.9–89.1 nm, with an average diameter of 19 nm. [Figure 3](#) shows that the highest differential number (34.2%) is attained for a diameter of 15.6 nm. The uniform size distribution of the CNFR isolated from ramie is similar to the results of [Chen et al. \(2011a\)](#); the primary difference being that they processed flax fibers using chemical-ultrasonication treatment.

FTIR spectroscopy analysis

[Figure 4](#) shows the FTIR spectra of the RR, PR, BR, and CNFR samples. The peaks at 3400–3300 cm^{-1} area scribed to stretching vibrations of OH, which indicate the hydrophilic properties of the material. The peaks at 2900–2800 cm^{-1} area attributed to asymmetric stretching caused by the C–H group ([Jonoobi et al. 2009](#)).

It can be seen from the FTIR spectra that there are no new functional groups present in the ramie fibers after the pulping and BRs. The peaks at 1625–1642 cm^{-1} area scribed to the bending mode of the absorbed water (O–H). It is evident from the FTIR spectrum for CNFR that the chemical-ultrasonication treatment has successfully reduced the amounts of hemicellulose and lignin in the ramie fibers since this peak disappears after treatment. In addition, it can be observed the intensity of the peak at 898 cm^{-1} increases after ultrasonication treatment (CNFR) compared with those for RR, PR, and BR samples. This indicates that the cellulose content is higher for the CNFR, as evidenced from the uptake of wave at 898 cm^{-1} , which is attributed to the presence of cellulose glucose ring ([Chirayil et al. 2014](#)).

XRD analysis

The XRD diffraction patterns were recorded for the RR, PR, BR, and CNFR samples in order to examine the crystallinity of the fibers at every stage of the chemical-ultrasonication treatment. The

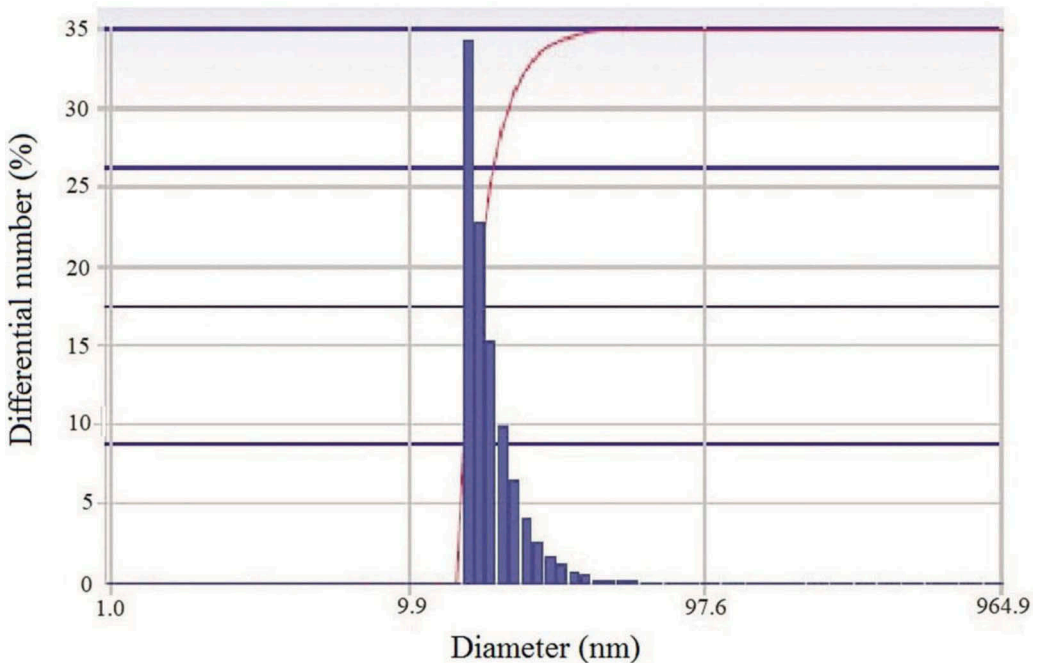


Figure 3. Distribution of diameter of the cellulose nanofibers.

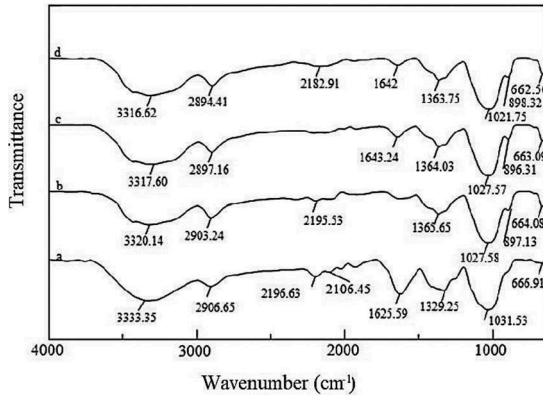


Figure 4. FTIR spectra of the (a) raw ramie fibers (RR), (b) ramie fibers after the pulping process (PR), (c) ramie fibers after the two-stage bleaching process (BR), and (d) cellulose nanofibers (CNFR).

crystalline indexes of the samples were determined using Eq.(2). The crystalline indexes of the RR, PR, BR, and CNFR samples are found to be 55.48%, 57.06%, 62.50%, and 73.65% for the RR, PR, BR, and CNFR samples, respectively, as shown in Table 2. Indeed, the crystallinity of ramie fibers is influenced by each process used to isolate the CNFR from RR fibers. The crystalline index increases to 57.06% after the PR, which may be due to the dispersion and removal of noncellulosic components (including hemicellulose and lignin) present in the amorphous phases of the RR fibers (George and Narayanankutty 2016). The crystalline index increases to 62.50% after the two-stage BR, which is due to the elimination of the remaining lignin. The crystalline index increases further to 73.65% after ultrasonication, indicating that ultrasonication contributes to homogenization and removal of the amorphous phase of the CNFR (Chen et al. 2011a). The results conform to the FTIR spectra and the results are similar to those obtained by Chen et al. (2011b), who isolated CNFR from wood.

Figure 5 shows the X-ray diffractograms of the RR, PR, BR, and CNFR samples. The peaks at $2\theta = 15.71^\circ, 22.34^\circ,$ and 32.00° for the RR sample indicate a typical cellulose I structure (Liu et al. 2007). Based on the Powder Diffraction FileTM by the Joint Committee on Powder Diffraction Standards (JCPDS), the RR sample has a monoclinic crystal structure with the following dimensions: $a = 6.74 \text{ \AA}, b = 5.93 \text{ \AA}, c = 10.36 \text{ \AA},$ and $\gamma = 810^\circ$. After chemical-ultrasonication treatment, the peaks have shifted to $2\theta = 12.01^\circ, 19.83^\circ,$ and 21.96° , indicating that the CNFR sample has a typical cellulose II structure. Based on the results, it is apparent that the chemical-ultrasonication treatment transforms the cellulose structure of the RR fibers from cellulose I to cellulose II structure (Liu et al. 2007). According to JCPDS Powder Diffraction FileTM, the CNFR sample has a crystal structure with the following dimensions: $a = 7.87 \text{ \AA}, b = 10.31 \text{ \AA},$ and $c = 10.13 \text{ \AA},$ and $\gamma = 900^\circ$.

TGA

It is crucial to conduct TGA of reinforcing materials in order to determine the applicability of these materials for bio composite processing at high temperatures. Figure 6 shows the thermograms of the

Table 2. Crystalline indexes of the raw ramie fibers (RR), ramie fibers after the pulping process (PR), and ramie fibers after the two-stage bleaching process (BR), and cellulose nanofibers (CNFR).

Sample	Crystalline index (%)
RR	55.48
PR	57.06
BR	62.50
CNFR	73.65

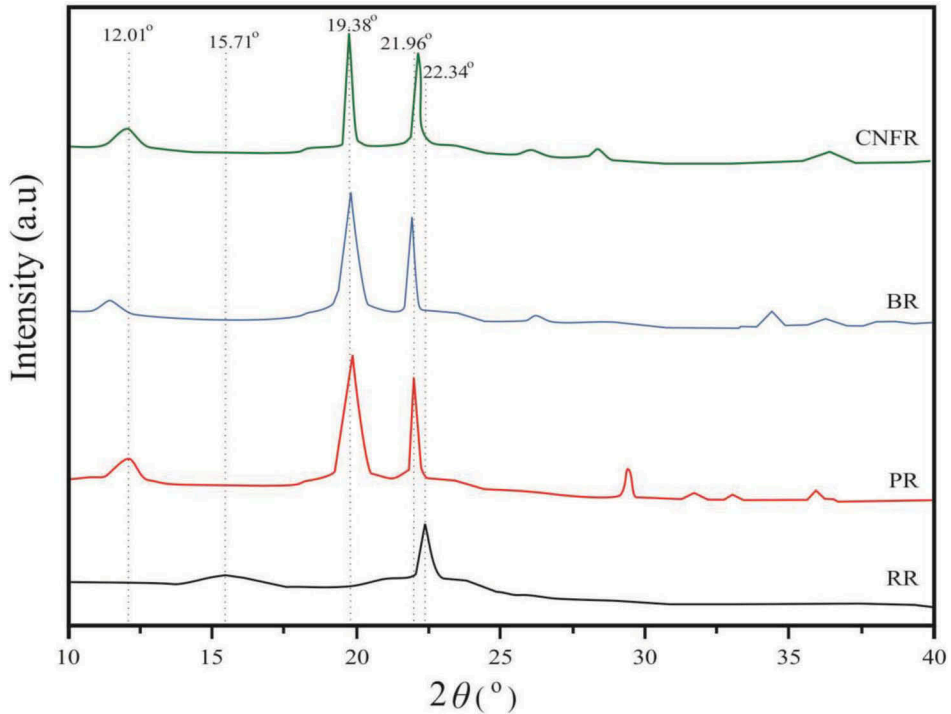


Figure 5. X-ray diffraction patterns of the raw ramie fibers (RR), ramie fibers after the pulping process (PR), ramie fibers after the two-stage bleaching process (BR), and cellulose nanofibers (CNFR).

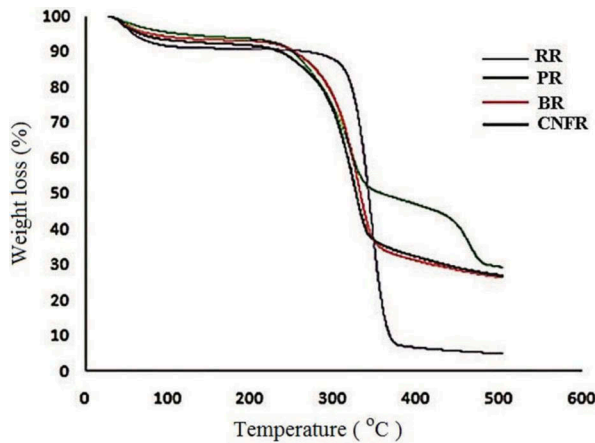


Figure 6. TGA curves of the raw ramie fibers (RR), ramie fibers after the pulping process (PR), ramie fibers after the two-stage bleaching process (BR), and cellulose nanofibers (CNFR).

RR, PR, BR, and CNFR samples obtained from the thermogravimetric analyzer. It can be seen that the CNFR sample has the highest thermal stability, followed by the BR, PR, and RR samples. The CNFR sample is characterized by the most pronounced weight loss of the residual ramie fibers at $\sim 350^\circ\text{C}$. In general, the thermal decomposition of the cellulosic components takes place within a temperature range of $200\text{--}400^\circ\text{C}$.

Table 3. Yield of cellulose nanofibers at a temperature of 70°C.

Ultrasonication treatment time (min)	Yield (%)
0 *	—
30	83.90
60	89.35

*An ultrasonication treatment time of 0 min indicates that the sample consists of native cellulose fibers obtained from the chemical treatment.

The initial thermal decomposition of lignocellulose has a negligible effect on the thermal decomposition of cellulose at various levels of treatment. The initial weight loss occurs within a range of 50–200°C, which may be due to the evaporation and removal of water (Wang, Shankar, and Rhim 2017). The carbon residue is ~27% for the RR, PR, and BR samples at 500°C, whereas the carbon residue is less than 10% for the CNFR sample. The material residues are higher in the RR sample compared with the other samples, which are expected because RR fibers contain high amounts of ash and lignin, which have a low degradation rate (Manfredi et al. 2006; Morán et al. 2008).

Yield of CNFR

The yield of the CNFR was calculated using Eq. (1) based on the thermogravimetric measurements and the results are tabulated in Table 3. It can be seen that an ultrasonication treatment time of 30 and 60 min results in a yield of 83.90% and 89.35%, respectively. The cellulose nanofiber yield obtained an ultrasonication time of 60 min is greater than that (85%) achieved by Habibi et al. (2008), which corresponds to a difference of 4.35%. They produced CNFR from ramie using the polycaprolactone-grafted method.

Conclusions

In this study, CNFR were successfully isolated from ramie (*Boehmerianivea* (L.) Gaud) using chemical-ultra sonication treatment. The average diameter and length of the CNFR are found to be 19 nm and 1 µm, respectively. Based on the chemical compositions of the RR, PR, and BR samples, there is a significant decrease in the hemicellulose and lignin content after the pulping and two-stage BRs. The absorbance peaks at 897 cm⁻¹ in the FTIR spectra indicate an increase in the cellulose content. Based on the TGA results, the CNFR isolated from ramie has the highest thermal stability. Based on the results of the XRD analysis, the crystalline index increases from 55.4% (RR) to 73.65% (CFNR). It can be concluded that chemical treatment (pulping and two-stage BRs) followed by ultrasonication is effective to isolate CNFR from ramie with a high yield of 89.39%.

Funding

This work was financially supported by Ministry of Research, Technology and Higher Education of the Republic of Indonesia (No. 1543 /PL.25/PL/2017).

References

- Abe, K., S. Iwamoto, and H. Yano. 2007. Obtaining cellulose nanofibers with a uniform width of 15 nm from wood. *Biomacromolecules* 8:3276–78. doi:10.1021/bm700624p.
- Abraal, H., D. Kadriadi, A. Rodianus, P. Mastariyanto, I. S. Arief, S. M. Sapuan, and M. R. Ishak. 2014. Mechanical properties of water hyacinth fibers – polyester composites before and after immersion in water. *Materials & Design* 58:125–29. doi:10.1016/j.matdes.2014.01.043.

- Benini, K. C. C. C., H. J. C. Voorwald, M. O. H. Cioffi, A. C. Milanese, and H. L. Ornaghi, JR. 2016. Characterization of a new lignocellulosic fiber from Brazil: Imperata brasiliensis (Brazilian Satintail) as an alternative source for nanocellulose extraction. *Journal of Natural Fibers* 14 (1):112–25. doi:10.1080/15440478.2016.1167647.
- Cadena, C. E. M., J. M., R. Vélez, J. F. Santa, and V. Otálvaro G. 2017. Natural fibers from plantain pseudostem (Musa Paradisiaca) for use in fiber-reinforced composites. *Journal of Natural Fibers* 14 (5):1–13. doi:10.1080/15440478.2016.1266295.
- Chen, W., H. Yu, Y. Liu, P. Chen, M. Zhang, and Y. Hai. 2011a. Individualization of cellulose nanofibers from wood using high-intensity ultrasonication combined with chemical pretreatments. *Carbohydrate Polymers* 83 (4):1804–11. doi:10.1016/j.carbpol.2010.10.040.
- Chen, W. S., H. P. Yu., P. Chen, N. X. Jiang, J. H. Shen, Y. X. Liu, and Q. Li. 2011b. Preparation and morphological characteristics of cellulose micro/nano fibrils. *Materials Science Forum* 675–677:255–58. doi:10.4028/www.scientific.net/MSF.675-677.
- Cherian, B. M., A. L. Leão, S. F. De Souza, S. Thomas, L. A. Pothan, and M. Kottaisamy. 2010. Isolation of nanocellulose from pineapple leaf fibres by steam explosion. *Carbohydrate Polymers* 81 (3):720–25. doi:10.1016/j.carbpol.2010.03.046.
- Chirayil, C. J., J. Joy, L. Mathew, M. Mozetic, J. Koetz, and S. Thomas. 2014. Isolation and characterization of cellulose nanofibrils from helicteres isora plant. *Industrial Crops and Products* 59:27–34. doi:10.1016/j.indcrop.2014.04.020.
- Damanik, N., H. C. Ong, W. T. Chong, and A. S. Silitonga. 2017. Biodiesel production from Calophyllum inophyllum–palm mixed oil. *Particle A: Recovery, Utilization, and Environmental Effects* 39 (12):1283–89.
- George, C. S., J. C., N., and S. K. Narayanankutty. 2016. Isolation and characterization of cellulose nanofibrils from areca nut husk fibre. *Carbohydrate Polymers* 142:158–66. doi:10.1016/j.carbpol.2016.01.015.
- Gopinath, R., K. Ganesan, S. S. Saravanakumar, and R. Poopathi. 2016. Characterization of new cellulosic fiber from the stem of sida rhombifolia. *International Journal of Polymer Analysis and Characterization* 21 (2):123–29. doi:10.1080/1023666X.2016.1117712.
- Habibi, Y., A.-L. Goffin, N. Schiltz, E. Duquesne, P. Dubois, and A. Dufresne. 2008. Bionanocomposites based on poly (Caprolactone) grafted cellulose nanocrystals by ring opening polymerization. *Journal of Materials Chemistry* 18 (41):5002–10. doi:10.1039/b809212e.
- Han, J., C. Zhou, A. D. French, G. Han, and Q. Wu. 2013. Characterization of cellulose ii nanoparticles regenerated from 1-butyl-3-methylimidazolium chloride. *Carbohydrate Polymers* 94 (2):773–81. doi:10.1016/j.carbpol.2013.02.003.
- Jonoobi, M., K. O. Niska, J. Harun, and M. Misra. 2009. Chemical composition, crystallinity, and thermal degradation of bleached and unbleached kenaf bast (Hibiscus Cannabinus) pulp and nanofibers. *BioResources* 4 (3):629–39.
- Khawas, P., and S. C. Deka. 2016. Isolation and characterization of cellulose nanofibers from culinary banana peel using high-intensity ultrasonication combined with chemical treatment. *Carbohydrate Polymers* 137:608–16. doi:10.1016/j.carbpol.2015.11.020.
- Kusumo, F., A. S. Silitonga, H. C. Ong, H. H. Masjuki, and T. M. I. Mahlia. 2017. A comparative study of ultrasound and infrared transesterification of *Sterculia foetida* oil for biodiesel production. *Energy Sources, Particle A: Recovery, Utilization, and Environmental Effects* 39 (13):1339–46. doi:10.1080/15567036.2017.1328003.
- Liu, Z.-T., Y. Yang, L. Zhang, Z.-W. Liu, and H. Xiong. 2007. Study on the cationic modification and dyeing of ramie fiber. *Cellulose (London, England)* 14 (4):337–45. doi:10.1007/s10570-007-9117-0.
- Lu, Y., and L. Cao, and Xiaodong. 2006. Morphological, thermal and mechanical properties of ramie crystallites reinforced plasticized starch biocomposites. *Carbohydrate Polymers* 63 (2):198–204. doi:10.1016/j.carbpol.2005.08.027.
- Manfredi, L. B., E. S. Rodríguez, M. Wladyka-Przybylak, and A. Vázquez. 2006. Thermal degradation and fire resistance of unsaturated polyester, modified acrylic resins and their composites with natural fibres. *Polymer Degradation and Stability* 91 (2):255–61. doi:10.1016/j.polymdegradstab.2005.05.003.
- Manimaran, P., P. Sentharamaikannan, K. Murugananthan, and M. R. Sanjay. 2017. Physicochemical properties of new cellulosic fibers from Azadirachta indica plant. *Journal of Natural Fibers* 15 (1):29–38. doi:10.1080/15440478.2017.1302388.
- Morán, J. I., V. A. Alvarez, V. P. Cyrus, and A. Vázquez. 2008. Extraction of cellulose and preparation of nanocellulose from sisal fibers. *Cellulose (London, England)* 15 (1):149–59. doi:10.1007/s10570-007-9145-9.
- Quintana, E., M. B. Roncero, T. Vidal, and C. Valls. 2017. Cellulose oxidation by laccase-tempo treatments. *Carbohydrate Polymers* 157:1488–95. doi:10.1016/j.carbpol.2016.11.033.
- Santhanam, K., A. Kumaravel, S. S. Saravanakumar, and V. P. Arthanarieswaran. 2016. Characterization of new natural cellulosic fiber from the ipomoea staphylyna plant. *International Journal of Polymer Analysis and Characterization* 21 (3):267–74. doi:10.1080/1023666X.2016.1147654.
- Segal, L., J. J. Creely, A. E. Martin Jr., and C. M. Conrad. 1959. An empirical method for estimating the degree of crystallinity of native cellulose using x-ray diffractometer. *Journal Text Researcher* 29:786–94. doi:10.1177/004051755902901003.

- Senthamarikannan, P., S. S. Saravanakumar, V. P. Arthanarieswaran, and P. Sugumaran. 2016. Physicochemical properties of new cellulosic fibers from bark of *Acacia planifrons*. *International Journal of Polymer Analysis and Characterization* 21:207–13. doi:10.1080/1023666X.2016.1133138.
- Silitonga, A. S., H. H. Masjuki, T. M. I. HwaiChyuanOng, and M. F. Kusumo. 2017. Optimization of extraction of lipid from *Isochrysisgalbana* microalgae species for biodieselsynthesis. *Energy Sources, Particle A: Recovery, Utilization, and Environmental Effects*. doi:10.1080/15567036.2017.1310957.
- Syafri, E., A. Kasim, H. Abrial, and A. Asben. 2017. Effect of precipitated calcium carbonate on physical, mechanical and thermal properties of cassava starch bioplastic composites. *International Journal on Advanced Science, Engineering and Information Technology* 7 (5):1950–56. doi:10.1851/ijaseit.7.5.1292.
- Syafri, E., A. Kasim, H. Abrial, A. Asben, and S. Wahono. 2016. Pengembangan digester pulp untuk menghasilkan partikel selulosa serat rami sebagai filler material bionanokomposit. *Prosiding Seminar Nasional Di Payakumbuh* 12. 12. Sept 2016:527–540. ISBN : 978-979-986910.
- Tibolla, H., F. M. Pelissari, M. I. Rodrigues, and F. C. Menegalli. 2017. Cellulose nanofibers produced from banana peel by enzymatic treatment: Study of process conditions. *Industrial Crops and Products* 95:664–74. doi:10.1016/j.indcrop.2016.11.035.
- Vignesh, V., A. N. Balaji, and M. K. V. Karthikeyan. 2016. Extraction and characterization of new cellulosic fibers from Indian mallow stem: An exploratory investigation. *International Journal of Polymer Analysis and Characterization* 21 (6):504–12. doi:10.1080/1023666X.2016.1175206.
- Wahono, S., A. Irwan, E. Syafri, and M. Asrofi. 2018. Preparation and characterization of ramie cellulose nanofibers/ CaCO_3 unsaturated polyester resin composites. *ARPN Journal of Engineering and Applied Sciences* 13 (2):746–51.
- Wang, L.-F., S. Shankar, and J.-W. Rhim. 2017. Properties of alginate-based films reinforced with cellulose fibers and cellulose nanowhiskers isolated from mulberry pulp. *Food Hydrocolloids* 63:201–08. doi:10.1016/j.foodhyd.2016.08.041.
- Yongvanich, N. 2015. Isolation of nanocellulose from pomelo fruit fibers by chemical treatments. *Journal of Natural Fibers* 12 (4):323–31. doi:10.1080/15440478.2014.920286.